Strain distributions in group IV and III-V semiconductor quantum dots

K. A. I. L. Wijewardena Gamalath, M. A. I. P. Fernando

Department of Physics, University of Colombo, Colombo 3, Sri Lanka

Email address: imalie@phys.cmb.ac.lk

ABSTRACT

A theoretical model was developed using Green's function with an anisotropic elastic tensor to study the strain distribution in and around three dimensional semiconductor pyramidal quantum dots formed from group IV and III-V material systems namely, Ge on Si, InAs on GaAs and InP on AlP. A larger positive strain in normal direction which tends to zero beyond $6nm$ was observed for all three types while the strains parallel to the substrate were negative. For all the three types of quantum dots hydrostatic strain and biaxial strain along x and z directions were not linear but described a curve with a maximum positive value near the base of the quantum dot. The hydrostatic strain in x-direction is mostly confined within the quantum dot and practically goes to zero outside the edges of the quantum dot. For all the three types, the maximum hydrostatic and biaxial strains occur in x-direction around $-1nm$ and around $2nm$ in z-direction. The negative strain in x-direction although realtively weak penetrate more deeper to the substrate than hydrostatic strain.The group IV substrate gave larger hydrostatic and biaxial strains than the group III-V semiconductor combinations and InAs /GaAs was the most stable. The results indicated that the movements of atoms due to the lattice mismatch were strong for group III-V.

Keywords: Quantum dot, strain distribution, hydrostatic strain, biaxial strain

1. INTRODUCTION

Tremendous amount of research has been devoted in the last two decade to the study of quantum confined structures. The research in semiconductor electronics on one-dimensional quantum wires had attained much attention with the exploration of carbon nanotubes. The end of the reduction of dimensionality was finally reached with the zero-dimension. Quantum dots are nanostructures whose spatial extents in all three dimensions are small enough so that they exhibit in some respect, quasi-zero-dimensional electronic properties. With the reduction of the dimensions, the conduction band and the valence band converts to square like energy band in quantum well and at zero-dimension, discrete energy levels are present (figure1).

Semiconductor material clusters, whose characteristic dimensions become comparable with the exciton Bohr radius, termed quantum dots, have real physical interpretation as zero-dimensional potential wells. The well defined number of electrons in these nanometer scale shapes may be adjusted by changing their elastic and electrostatic environment.

Figure 1. Energy band structure for zero, one, two, three dimensions with the size
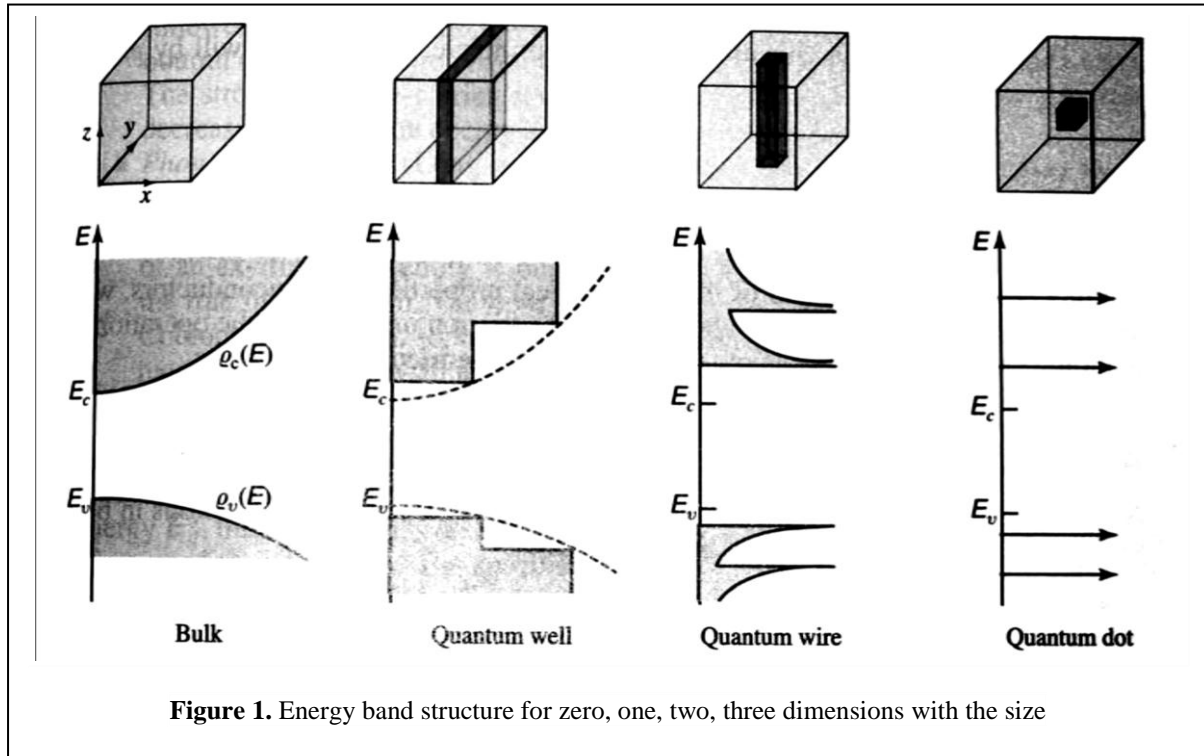
As quantum dots can be considered as a tiny crystals acting as one very large artificial atom, these are of considerable interest from a purely scientific standpoint as they can be distinguished by their discrete energy spectrum sharing the properties of single atoms which can be used as "artificial" atoms to test fundamental theories of the atomic physics. Although several technological barriers still remain semiconductor quantum dots are of immense technological importance and are often considered as basis for several revolutionary nanoelectronic devices such as low-threshold optoelectronic devices as well as for quantum computing applications. They can exist in a wide variety of shapes, including cubical, pyramidal, truncated-pyramidal and lens-shaped. The phenomenon of strain-mediated self-assembly has particularly been the subject of intensive investigations as a versatile nanofabrication tool by which a variety of coherent and defect free semiconductor quantum dots and nanowires can be prepared inspiring a wide spectrum of potential nanoscale technologies[1]. Continuum elasticity and atomistic elasticity are the two approaches used to study the strains in quantum dots. In continuum elasticity, elastic energy is considered in terms of strain energy whereas in atomistic elasticity elastic energy is considered in terms of body potentials between atoms. Comparing these two methods, Prior[2] related the strain in the substrate material to the strain in the quantum dot. A simple method involving the evaluation of a surface integral over the boundary of the quantum dot was used by Downs et al[3] for calculating the stress and strain distributions arising from an initially uniformly strained quantum dot of arbitrary shape buried in an infinite isotropic medium. The strain distributions in quantum dots using Green's functions with Fourier transformations was used by Andreev et al[4] to obtain strain tensor for arrays of anisotropic quantum dots. Analytical solution for isotropic strain distributions using Green's functional method with isotropic Green's tensor was obtained by Faux and Pearson[5]. For successive orders of corrections this model converges towards an anisotropic model. Maranganthi and Sharma[6] used a Green's functional approach to calculate strain fields in embedded quantum dots and wires. Using classical theories and Green's function method, Wang et al[7] obtained a general solution for strain

profile for arbitrary shaped quantum dots and analyzed the quantum dot induce strain and electric fields in piezoelectric semiconductors.

In the present work, the Green's functional approach of Maranaganthi and Wang[6,7] was extended by including three dimensional anisotropic strain tensor to find the strain in and around any general shape of semiconductor quantum dot. Anisotropy was included by a new equation which combines the isotropic elasticity and the anisotropic constant. The displacement was derived using Cartesian coordinate system for a pyramidal shaped quantum dot. Throughout the analysis of the strain profiles, base length and the height of the pyramid were kept as constants. For three types of quantum dot materials formed from group IV, Si on Ge and group III-V material systems, InAs on GaAs and InP on AlP, the stain tensor components as well as hydrostatic and biaxial strain distributions in the x and z directions were plotted. Group IV semiconductor strain induced quantum dots are interesting due to their compatibility with mainstream semiconductor industry and also due to their simplicity from the fundamental science standpoint. Due to smaller lattice mismatch (4%) between Si and Ge pure (intrinsic) semiconductors, Ge/Si quantum dots are suitable for detailed characterization with high resolution atomic force microscopes and scanning tunneling microscopes[8]. Also the extraction processes are comparably easier compared to compounds like GaAs/InAs, InP/AlP. GaAs/InAs been one of the most extensively investigated systems is of particular technological interest due to the high optical efficiency that can be realized.

2. STRAIN TENSOR FOR PYRAMIDAL QUANTUM DOTS

It is generally accepted that strain is the primary factor for quantum dot formation in lattice mismatched semiconductor systems.

Quantum dot is created when a thin layer of a semiconductor or a metal material known as wetting layer is deposited on a substrate material which has lower lattice constant (Figure 2). Because of the lattice mismatch between substrate
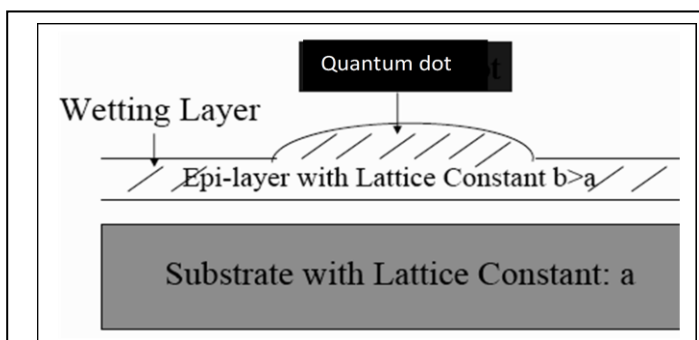
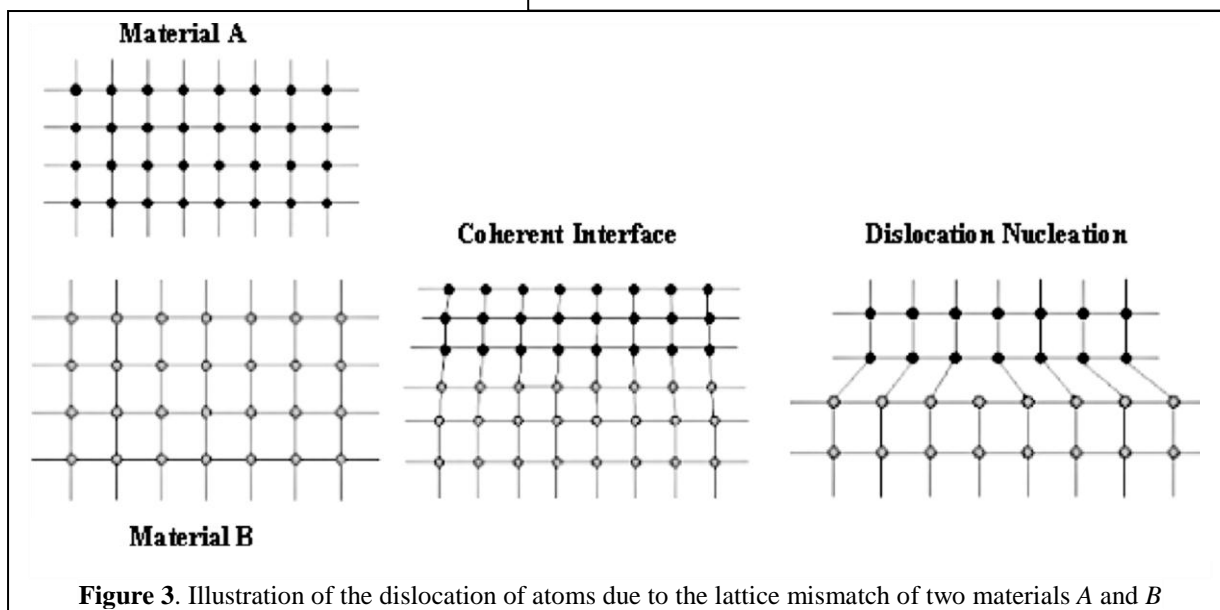**Figure 2**. Illustration of the growth process of wetting layer

Figure 3. Illustration of the dislocation of atoms due to the lattice mismatch of two materials *A* and *B*

material and the wetting material atoms in both quantum dot and substrate material try to relax elastically to accommodate this mismatch creating a body force. Atoms in wetting layer try to minimize the strain energy that is created by the perturbation of body force creating stretches and dilations in inter atomic bonds (Figure 3). The shape of the created quantum dot varies with the manufacturing method.

In elastic materials of two substrates with lattice constants a_1 and a_2 parallel to the interface, the lattice mismatch or eigenstrain e_{kl} whose effect generally similar to that of interface energy is given by

$$e_{kl} = \frac{(a_1 - a_2)}{a_1} \qquad (1)$$

and their representation by equivalent body force are well established in the classical micromechanics[9,10]. The elastic field is described by displacement vector u, stress tensor σ_{ij}, strain tensor ε_{kl} and the elastic constant also known as stiffness tensor C_{ijkl}

$$\sigma_{ij} = C_{ijkl}\left(\varepsilon_{kl} - e_{kl}\right) \qquad (2)$$

where, $i, j, k \in \{z, y, z\}$. The six independent strain tensor components consisting of diagonal components ε_{ii} representing the normal strain, compression or dilatation along the axes of the chosen coordinate system controlling the length of the axis and the non-diagonal shear strain components $\varepsilon_{ij}(i \neq j)$ controlling the angle between the axes are obtained from

$$\varepsilon_{ij} = \varepsilon_{ji} = \frac{1}{2}\left(\frac{\partial u_i}{\partial r_j} + \frac{\partial u_j}{\partial r_i}\right), \qquad \varepsilon_{ii} = \frac{\partial u_i}{\partial r_i} \qquad (3)$$

where $u = (u_x, u_y, u_z$ For small strains $\frac{\partial u_i}{\partial r_j} \gg 1$. Using the above symmetric conditions, equation 2 reads

$$\sigma_{ij} = C_{ijkl}\left(\frac{\partial u_k}{\partial r_l} - e_{kl}\right) = C_{ijkl}\left(u_{k,l} - e_{kl}\right). \qquad (4)$$

Substitution of equation 4 into equilibrium condition $\sigma_{ij,i} = 0$, leads to

$$C_{ijkl}\frac{\partial^2 u_k}{\partial r_i \partial r_l} = C_{ijkl}\frac{\partial e_{kl}}{\partial r_i}. \qquad (5)$$

The equivalent body force created by the lattice mismatch is[7]

$$f_i(\boldsymbol{r}) = -C_{ijkl}e_{kl,i} \qquad (6)$$

The above equation leads to a volume integral representation of the displacement

$$u_p(\boldsymbol{r}) = -\int_V G_{jp}(\boldsymbol{r},\boldsymbol{r}')\left[C_{ijkl}e_{kl}\right]_{,i} dV(\boldsymbol{r}') \quad (j,p \in \{x,y,z\}) \qquad (7)$$

The Green's function $G_{jp}(\boldsymbol{r},\boldsymbol{r}')$ is a singular displacement solution produced by a point source corresponding to j^{th} component of extended displacement at location $\boldsymbol{r}$ produced by the pth component of an extended point force applied at $\boldsymbol{r}'$. By assuming that the eigenstrain is uniform within the quantum dot domain *V*, the volume integral can be transformed into surface integral on the boundary ΔV using Gauss's theorem

$$u_p(\boldsymbol{r}) = C_{ijkl}e_{kl}\int_{\Delta V} G_{jp}(\boldsymbol{r},\boldsymbol{r}')n_i(\boldsymbol{r}) ds(\boldsymbol{r}') \qquad (8)$$

where $n_i(\boldsymbol{r})$ is the outward normal to the boundary ΔV. Green's function for Navier's equation is given by[6]

$$G_{ij}(r) = \frac{1}{8\pi(\lambda+2\mu)}\left[(\lambda+3\mu)\frac{\delta_{ij}}{|r|}+(\lambda+\mu)\frac{r_i r_j}{|r|^3}\right] \qquad (9)$$

where $|r_i| = r_i$ and the elastic tensor is expressed in terms of two Lame constants (λ,μ), λ representing the bulk modulus and μ the sheer modulus. A pyramid can be considered to be formed by four triangular planes with a base (Figure 4) and the equations of the four triangular planes are derived by using two equations for any triangular plane with the direction ratios of a line perpendicular to that particular plane. The equation of the *ABE* plane is given by

$$x-y+\left(\frac{a}{h\sqrt{2}}\right)z-\left(a/\sqrt{2}\right) = 0 \quad \begin{cases} 0 \le x \le a/\sqrt{2} \\ 0 \le y \le a/\sqrt{2} \\ 0 \le z \le h \end{cases} \qquad (10)$$

Similarly, the equations for *BCE, DCE* and *ADE* planes and z direction are respectively

$$x + y + \left(\frac{a}{h\sqrt{2}}\right)z - \left(a\Big/\sqrt{2}\right) = 0,$$

$$x - y - \left(\frac{a}{h\sqrt{2}}\right)z + \left(a\Big/\sqrt{2}\right) = 0,$$

$$x + y - \left(\frac{a}{h\sqrt{2}}\right)z + \left(a\Big/\sqrt{2}\right) = 0,$$

$$z = \frac{h\sqrt{2}}{a}\left\{\frac{a}{\sqrt{2}} - \left(|x|+|y|\right)\right\}. \qquad (11)$$

The general position coordinate read,

$$\mathbf{r} = x\mathbf{i} + y\mathbf{j} + \frac{h\sqrt{2}}{a}\left\{\frac{a}{\sqrt{2}} - \left(|x|+|y|\right)\right\}\mathbf{k}. \qquad (12)$$

Figure 4 (*a*). InAs/GaAs quantum dot.

Figure 4(*b*). Geometrical representation of coordinates of a pyramid

By assuming that quantum dot surface can be effectively represented by number of triangular surfaces, displacements can be obtained from the equation 8 which in matrix form read,

$$
\begin{bmatrix} u_x \\ u_y \\ u_z \end{bmatrix} =
\begin{bmatrix}
\iint C_{ixkl}e_{kl}G_{xx}dxdy & \iint C_{iykl}e_{kl}G_{xy}dxdy & \iint C_{izkl}e_{kl}G_{xz}dxdy \\
\iint C_{ixkl}e_{kl}G_{xy}dxdy & \iint C_{iykl}e_{kl}G_{yy}dxdy & \iint C_{izkl}e_{kl}G_{yz}dxdy \\
\iint C_{ixkl}e_{kl}G_{zy}dxdy & \iint C_{iykl}e_{kl}G_{zy}dxdy & \iint C_{izkl}e_{kl}G_{zz}dxdy
\end{bmatrix} \qquad (13)
$$

In the isotropic case, the elasticity constant can be written as,

$$C_{ijkl} = K\delta_{ij}\delta_{kl} + U\left(\delta_{ij}\delta_{jl} + \delta_{il}\delta_{jk} - \frac{2}{3}\delta_{ij}\delta_{kl}\right) \qquad (14)$$

Where K is the bulk modulus, U is the shear modulus and δ is the kronecker delta function. Using the derivatives of displacement vectors obtained in equation 13 in equation 3, the strain tensor components can be obtained. In anisotropic media, the elasticity tensor gives the relationship between stresses and strains. As the symmetry of stress tensor indicates that there are at most six different elements of stress, the fourth rank elasticity tensor C_{ijkl} can be written as a second rank matrix using Voigt notation,
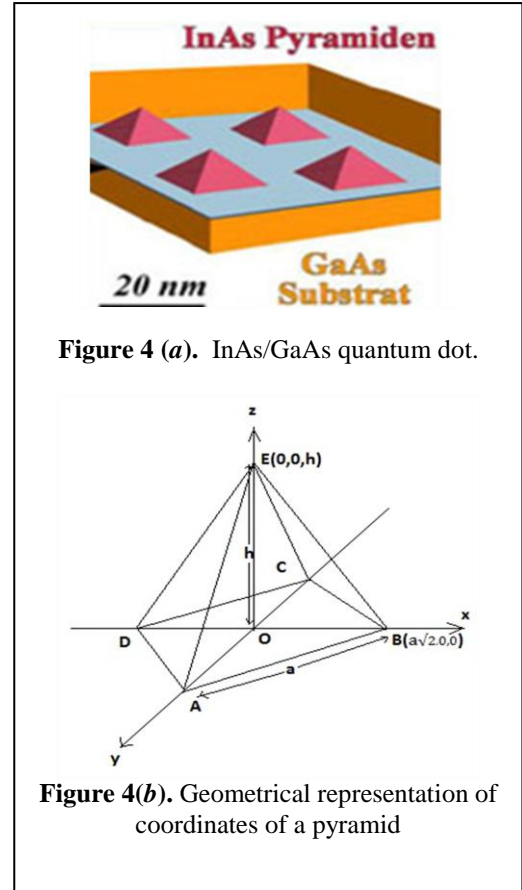
$$ij = 11 \quad 22 \quad 33 \quad 23,32 \quad 13,31 \quad 12,21$$
$$\Downarrow \quad \Downarrow \quad \Downarrow \quad \Downarrow \quad \Downarrow \quad \Downarrow \quad \Downarrow$$
$$\alpha = 1 \quad 2 \quad 3 \quad 4 \quad 5 \quad 6$$

$$C_{\alpha\beta} = \begin{bmatrix} K+4U/3 & K+2U/3 & K+2U/3 & 0 & 0 & 0 \\ K+2U/3 & K+4U/3 & K+2U/3 & 0 & 0 & 0 \\ K+2U/3 & K+2U/3 & K+4U/3 & 0 & 0 & 0 \\ 0 & 0 & 0 & U & 0 & 0 \\ 0 & 0 & 0 & 0 & U & 0 \\ 0 & 0 & 0 & 0 & 0 & U \end{bmatrix} \tag{15}$$

3. STRAIN PROFILES FOR Ge/Si, InAs/GaAs AND InP/AlP QUANTOM DOTS

With z axis directed normal to the hetero interface, the displacements in the three directions of the pyramidal quantum dot were obtained in Cartesian coordinates using equation 13 with the anistropic elastic tensor given in equation 15 and the strain components in equation 3.

In this case, the strain components along x and y axes are same due to symmetry, $\varepsilon_{xx} = \varepsilon_{yy} = \varepsilon_\parallel$ and $\varepsilon_{zz} = \varepsilon_\perp$ where $\varepsilon_\parallel$ and $\varepsilon_\perp$ are strain components in the directions parallel and normal to the plane of the hetero interface, respectively.

Hydrostatic strain and biaxial strain have a crucial influence on the potential energy of electron, the light-wave splitting and the hole states, having a significant effect on the study of photoelectric properties of quantum devices. The hydrostatic strain component can be written as

$$\varepsilon_{hy} = \varepsilon_{xx} + \varepsilon_{yy} + \varepsilon_{zz} = \varepsilon_\parallel + \varepsilon_\perp \tag{16}$$

and the biaxial strain component as

$$\varepsilon_{bi} = \varepsilon_{zz} - \frac{1}{2}(\varepsilon_{xx} + \varepsilon_{yy}) = \varepsilon_\perp + \varepsilon_\parallel \tag{17}$$

Table 1. Lattice Constants and Crystal Structures of the Semiconductors

Element or Compound	Type	Name	Crystal Structure	Lattice Constant at 300 K (Å)
Ge	Element	Germanium	Diamond	5.64613
Si	Element	Silicon	Diamond	5.43095
InAs	III-V	Indium arsenide	Zincblende	6.0584
GaAs	III-V	Gallium arsenide	Zincblende	5.6533
InP	III-V	Indium phosphide	Zincblende	5.8686
AlP	III-V	Aluminum phosphide	Zincblende	5.4510

Three quantum dots formed from hetero structures of group IV, the low dimensional indirect gap semiconductors, Ge grown on Si, and III-V direct gap semiconductors InAs grown on GaAs, and direct gap InP grown on indirect gap AlP semiconductors were considered. The materials selected for the preparation of quantum dots mainly depend on their energy gap and their lattice mismatch. The lattice constants of these materials at 300^0K are tabulated in table 1 and lattice mismatch for the three quantum dots in table 2.

Table 2. Lattice mismatch

Quantum Dot	Lattice mismatch %
Ge/Si	3.9
InAs/GaAs	6.8
InP/AlP	7.2

The base length a of the pyramid (Figure 4) was taken as $15.5nm$ and the height h as $5.5nm$. All the graphs were obtained for x, y range of $-5nm$ to $+5nm$ and z range of $-4nm$ to $8nm$. The strain profiles for the three semiconductor quantum dots Ge/Si, InAs/ GaAs and AlP /InP materials in x and z directions are shown in Figure 5, 6 and 7 respectively. All the maximum and minimum strain values lie within the base length $a/\sqrt{2}$ ($\sim11nm$). A higher resultant strain is located in the lower half of the pyramid than in the upper half of the pyramid where the forces act mainly from the sides along the z direction. All three quantum dot combinations have large strain components normal to the plane and these strain components $\varepsilon_{xz}, \varepsilon_{yz}, \varepsilon_{zz}$ have positive strains or dilations inside the pyramid while the maximum dilation occur along the vertical axis of the pyramid (ε_{zz}). The stress close to the vertex of the quantum dot is a small compression, which changes into a rapidly increasing

tension along the path, and reaches a maximum at the interface. Following this, the stress is decreased in the substrate and tends to zero beyond *6nm* far from the interface, forming the effect of "far field".
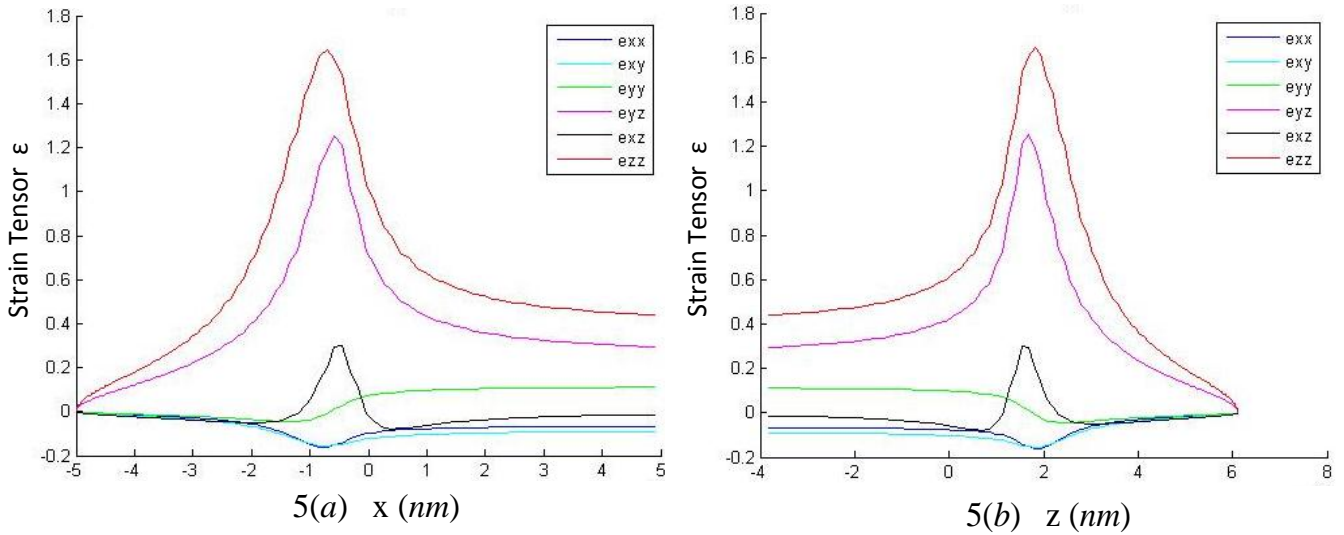

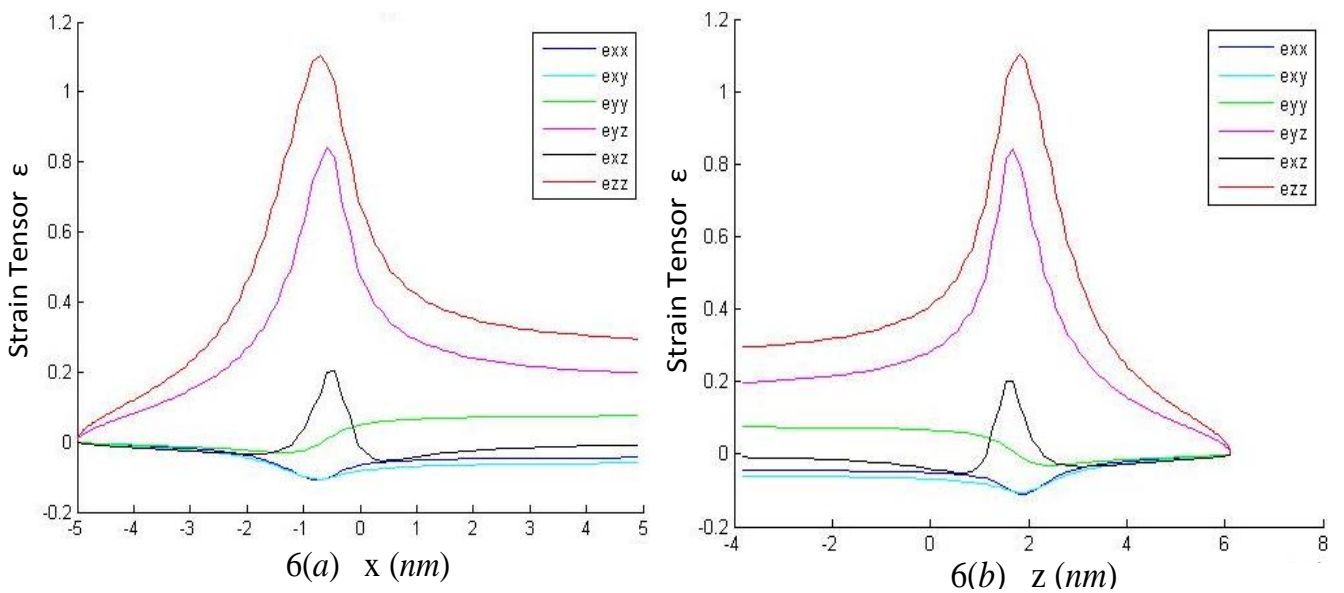**Figure 5.** Strain profile of Ge/Si (*a*) in x-direction and (*b*) in z-direction

Figure 6. Strain Profile of InAs/GaAs (*a*) in x-direction and (*b*) in z- direction

For all the three types of quantum dots, the parallel strain components in x-y plane $\varepsilon_{xx}, \varepsilon_{yy}, \varepsilon_{xy}$ along x and z directions have small negative values, indicating compression in these directions. These compressive strains were created near the base of the pyramids. The strain rapidly changed across the interface, such that the compression and contraction in the film are changed into tension and elongation in the substrate, respectively. The strains in the substrates are attenuated to zero far from the interfaces. The strain across the interface being changed from contraction to elongation shows the self-adjustability of epitaxial growth, i.e. the epitaxial material and substrate can choose respective deformation of each other to enforce a matched and coherent interface. For the pyramidal quantum dots, the group IV semiconductor materials substrate Ge/Si has larger dilations and compressions in the three directions compared to the quantum dots formed from the group III-V substrate materials. In group III-V substrates, InP/AlP have higher dilations and compressions than InAs/GaAs.
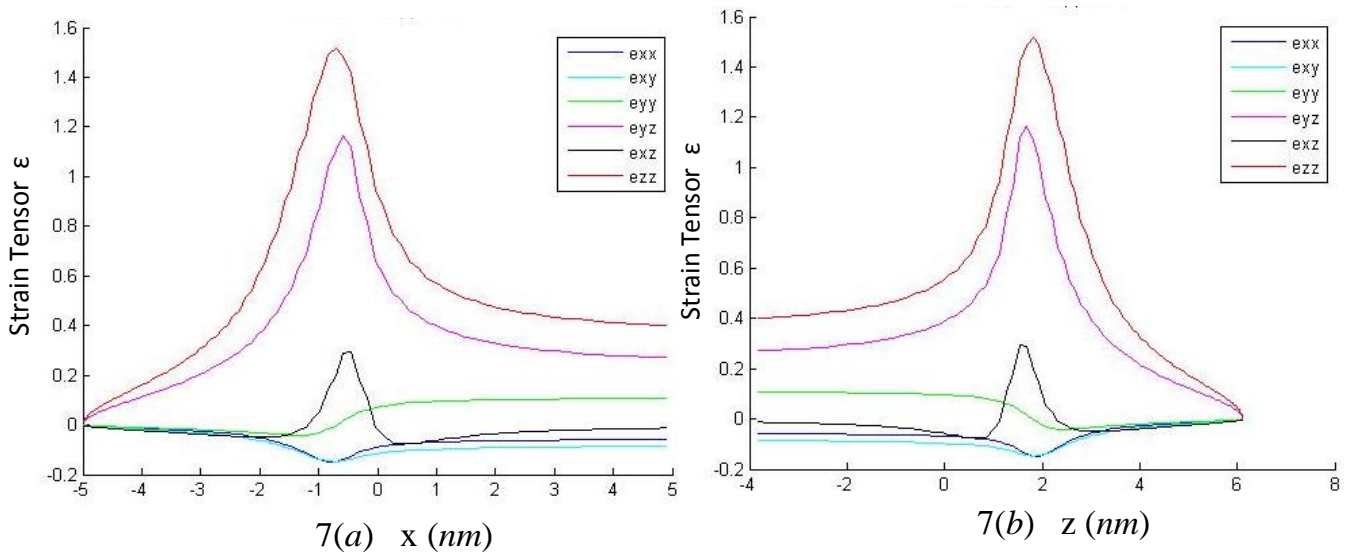

7(*a*)   x (*nm*)

7(*b*)   z (*nm*)

Figure 7. Strain Profile InP/AlP (*a*) in x-direction and (*b*) in z-direction
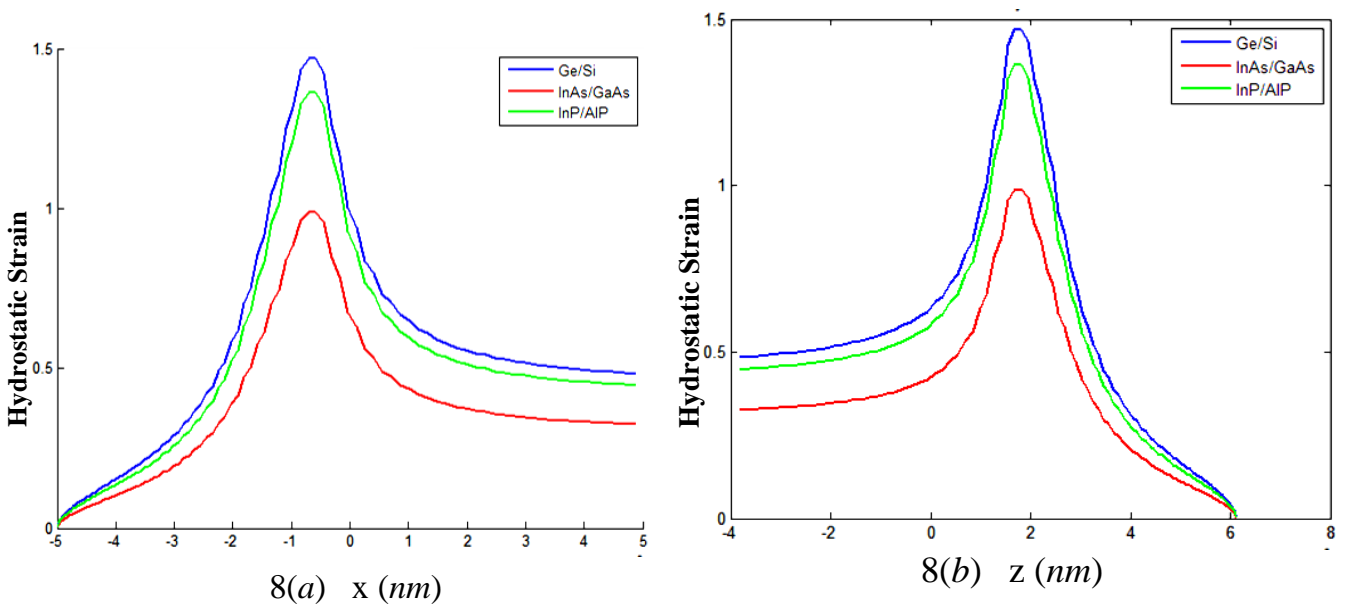

8(*a*)   x (*nm*)

8(*b*)   z (*nm*)

Figure 8. Hydrostatic strain for the three material systems (*a*) in x-direction and (*b*) in z-direction

The hydrostatic strain, biaxial strain and strain along along x and z directions for the three quantum dots are shown in figures 8 and 9 respectively. For all the three quantum dots the hydrostatic strain and biaxial strain are not linear but describe a curve with a maximum positive value. Group IV quantum dot has a higer hydrostatic and biaxial strain than Group III-V semiconductor substrate quantum dots while in group III-V material InP/AlP has higer values than InAs/GaAs.
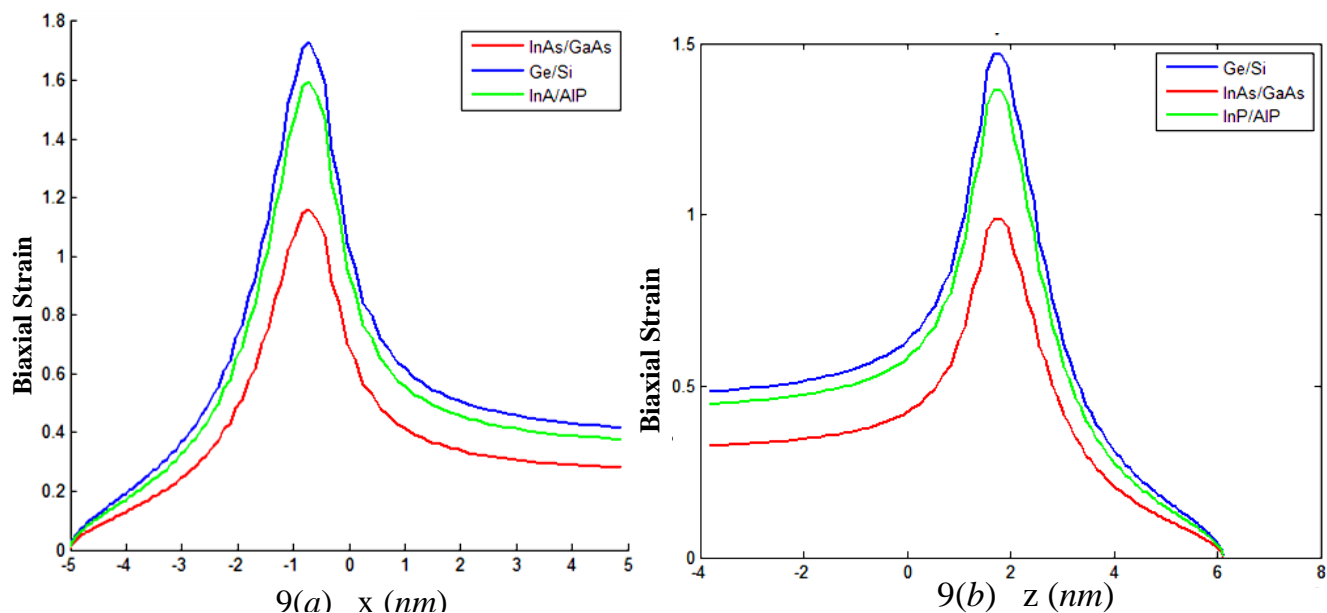

Figure 9. Biaxial strain for the three material systems (*a*) in x-direction and (*b*) in z-direction
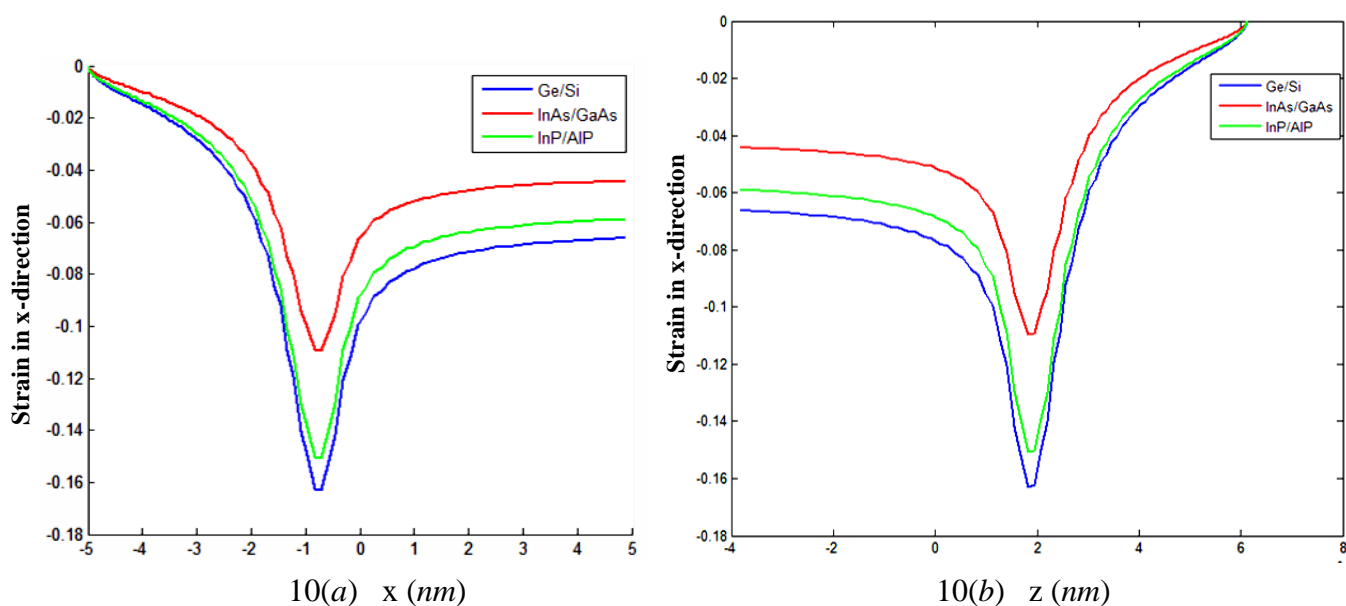

Figure 10. Strain along x-axis (*a*) in x-direction and (*b*) in z-direction for the three material systems

Hydrostatic and biaxial strain components are positive within the quantum dots. For all the three types, the maximum hydrostatic and biaxial strains in x-direction occur around -1.0 and $-0.5\,nm$ and goes to zero around $-5\,nm$ while in z direction, the maximum hydrostatic strain and biaxial strain occur around 1 and $2\,nm$ and practically goes to zero around $6\,nm$. The magnitude of hydrostatic and biaxial strain are particularly high near the base of the quantum dot. The negative parallel strain components along x-axis ε_{xx} are realtively weak compared to hydrostatic and biaxial strains (Figure 10).

4. CONCLUSION

For the pyramidal quantum dots, the group IV semiconductor materials substrate Ge grown on Si and III-V semiconductor material substrates InAs grown on GaAs and InP grown on AlP gave the same shapes for strain profiles along x and z axes. The higher dilation or positive strain components for all the three substrates were normal to the substrate indicating that the growth process in semiconductor quantum dots takes place in z direction due to the body forces created by the lattice mismatch.

To balance this effect and retain the equilibrium by minimizing the energy, the parallel strain components were negative with small values near the base of the pyramid, and approached zero with the height of the pyramid. Interchanging the two materials of the semiconductor in the quantum dot, compressive strains can be obtain in the x-y plane and dilative strains normal to the substrate. Near the base, the forces were exerted primarily parallel to the substrate plane and as the substrates try to force the wetting material lattice constants to approach that of the substrate, compressive strains were created along the z-axis. For all the three quantum dots hydrostatic and biaxial strain components were positive within the quantum dots acting strongly near the base of the pyramid.

The hydrostatic strain in x-direction is mostly confined within the quantum dot and practically goes to zero outside the edges of the quantum dot. The negative parallel strain along x-axis although relatively weak penetrate more deeper to the substrate than hydrostatic strain. A higher resultant strain was located in the lower half of the pyramid than in the upper half of the pyramid, the forces acting mainly from the sides along the normal direction. The strain field was not confined to the pyramid alone, but extended over a large region of the substrate material between the pyramid and the surface indicating that there is deformation in the wetting material as it spread in all directions.

The group IV indirect gap semiconductors Ge/Si substrate gave the largest dilations and compressions in all the directions than the other two III-V substrate combinations even though it had the lowest lattice mismatch (4%). In the group III-V the strain distribution for direct gap InP grown on in direct gap AlP was higher than direct gap semiconductors InAs grown on GaAs. InAs/GaAs has a lower lattice mismatch than Inp/AlP. Therefore these results indicated that the movements of atoms due to the lattice mismatch were stronger for group III-V. The most popular material InAs/GaAs have the lowest strain than the other two combinations maintaining the stability.

REFERENCES

1. J. Stangl, V. Holý, G. *Bauer, Rev. Mod. Phys.* 76 (2004) 725-783.

2. C. Prior, *Journal of Applied Physics* 83 (1997) 2548-2553.

3. J. R. Downs, D. A. Faux, E. P. O'reilly, *Journal of Applied Physics* 81 (1997) 6700-6702.

4. A. D. Andreev, J. R. Downs, D. A. Faux, E. P. O'reilly, *Journal of Applied Physics* 86 (1999) 297-305.

5. D. A. Faux, G. S. Pearson, *Journal of Applied Physics* 62 (2000) 4798-4801.
     G. S. Pearson, D. A. Faux, *Journal of Applied Physics* 88 (2000) 730-736.

6. R. Maranganthi, P. Sharma, *A Review of strain field calculation in embedded quantum dots and wires*, *Handbook of Theoretical and Computational Nanotechnology* Edited by Michael Rieth and Wolfram Schommers (American Scientific Publishers, 2005) Chapter 118, Volume 1: Pages (1–44). ISBN: 1-58883-042-X.

7. C. Y. Wang, M. Denda, E. Pan, *International Journal of Solids and Structures,* Vol. 43 (2006) 7593-7608.
     J. Chu, J. Wang, *Journal of Applied Physics* 98 (2005) 1-7.

8. S. A. Komarov, *Potential of strain induced semiconductor quantum dots for device applications*, Ph.D. thesis, Stanford University (2002).

9. J. D. Eshelby, *Elastic inclusions and inhomogeities,* Edited by I. N. Sneddon,

     R. Hill (North Holland, 1961), Progress in Solid Mechanics, Vol. 2 pp. 89-140.

10. T. Mura, *Micromechanics of defects in solids* (Martinus Nijhoff, Dordrecht,1987) 2nd edition.

11. L. D. Landau, E. M. Lifshitz, "*The Classical Theory of Fields*." (ButterworthHeinemann, 1980) Vol. 2.